

Titre: Collocated MIMO travelling wave SIW slot array antennas for millimetre waves

Auteurs: Asim Ghalib, Mohammad S. Sharawi, Raj Mittra, Hussein Attia, & Atif Shammim

Date: 2021

Type: Article de revue / Article

Référence: Ghalib, A., Sharawi, M. S., Mittra, R., Attia, H., & Shammim, A. (2021). Collocated MIMO travelling wave SIW slot array antennas for millimetre waves. IET Microwaves, Antennas & Propagation, 15(8), 815-826.
Citation: <https://doi.org/10.1049/mia2.12110>

Document en libre accès dans PolyPublie

Open Access document in PolyPublie

URL de PolyPublie: <https://publications.polymtl.ca/9302/>
PolyPublie URL:

Version: Version officielle de l'éditeur / Published version
Révisé par les pairs / Refereed

Conditions d'utilisation: CC BY
Terms of Use:

Document publié chez l'éditeur officiel

Document issued by the official publisher

Titre de la revue: IET Microwaves, Antennas & Propagation (vol. 15, no. 8)
Journal Title:



Maison d'édition: John Wiley & Sons
Publisher:

URL officiel: <https://doi.org/10.1049/mia2.12110>
Official URL:

Mention légale: © 2021 The Authors. IET Microwaves, Antennas & Propagation published by John Wiley & Sons Ltd on behalf of The Institution of Engineering and Technology. This is an open access article under the terms of the Creative Commons Attribution License, which permits use, distribution and reproduction in any medium, provided the original work is properly cited.
Legal notice:

ORIGINAL RESEARCH PAPER

Collocated MIMO travelling wave SIW slot array antennas for millimetre waves

Asim Ghalib¹  | Mohammad S. Sharawi² | Raj Mittra¹ | Hussein Attia³  | Atif Shammim⁴

¹Electromagnetic Communication Laboratory, University of Central Florida, Orlando, Florida, USA

²Department of Electrical Engineering and Poly-Grames Research Center, Polytechnique Montreal, Montreal, Canada

³Department of Electrical Engineering, King Fahd University of Petroleum and Minerals, Dhahran, Saudi Arabia

⁴Division of Computer, Electrical, Mathematical Science and Engineering, King Abdullah University of Science and Technology, Thuwal, Saudi Arabia

Correspondence

Asim Ghalib, Electromagnetic Communication Laboratory, University of Central Florida, Orlando, FL, USA.
Email: asim.ghalib@ucf.edu

Funding information

King Fahd University of Petroleum and Minerals, Grant/Award Number: FT161006; King Abdullah University of Science and Technology, Grant/Award Number: ST-2016-KKI-2899

Abstract

A novel four-element collocated travelling wave substrate integrated waveguide (SIW) multiple-input multiple-output (MIMO) antenna covering millimetre wave (mm-wave) bands (28–32 GHz) is presented. The antenna exhibits a matching bandwidth of more than 4 GHz and a measured gain of 15 dBi. The MIMO antenna elements are collocated, thus significantly reducing the size of the proposed design. To spatially isolate the beams (obtain lower correlation coefficient) of the MIMO antenna elements, the beams are oriented in different directions. The slots within each SIW array are designed to provide tilted beams, thus eliminating the need for a beam switching network. Four distinct beams are formed towards $\pm 10^\circ$ and $\pm 30^\circ$. The dimension of the four-element MIMO SIW design is $68 \times 30.68 \times 0.5 \text{ mm}^3$. The proposed antenna has a high gain, compact size, simpler feeding and enhanced MIMO capability compared to other SIW antennas proposed in the literature.

1 | INTRODUCTION

Multiple-input multiple-output (MIMO) technology is currently used in 4G enabled terminals because of its ability to provide enhanced data rates within limited bandwidth (BW) and power limits [1]. MIMO technology is also employed in 5G systems, with antennas operating at higher frequencies to provide wider BWs (needed to cover the data requirements), higher gains (to counter the atmospheric attenuation) and the ability to integrate with planar structures [2–5]. Antenna design at mm-waves is a challenging task and incorporating MIMO configurations makes it even more challenging.

Microstrip antennas suffer from high losses at mm-waves, and consequently, their gain is limited. A microstrip antenna as a single element normally has a relatively broad beam-width and high back lobe levels. Owing to these limitations, such antennas are normally used in array configuration to provide

enhanced gain. The feed network of the array helps to form and control the beam. The use of the array and its feed not only adds complexity to the design process, but also increases the size and associated losses. A three- and six-element MIMO planar inverted-F (PIFA) antennas operating at 28 GHz were presented in [6, 7] respectively, both with gains around dBi. A four-element MIMO antenna, where each element consisted of a connected array of eight PIFA sub-elements that are fed by a power divider, was presented in [8]. The connected array had a BW of 1 GHz and operated at 28 GHz. In [9], two multi-layer arrays were presented, where each array consisted of eight dipole elements operating at 28 GHz. The same configuration was also used with Bow-tie elements in [10]. A four-element T-shaped patch antenna with defected ground structures for enhanced BW and gain, operating at 29 GHz, was presented in [11]. 4G/5G integrated MIMO antenna systems for mobile handset devices were presented in [12–16].

This is an open access article under the terms of the Creative Commons Attribution License, which permits use, distribution and reproduction in any medium, provided the original work is properly cited.

© 2021 The Authors. *IET Microwaves, Antennas & Propagation* published by John Wiley & Sons Ltd on behalf of The Institution of Engineering and Technology.

Slot arrays based on substrate integrated waveguides (SIWs) offer an alternative to microstrip based antenna arrays, since they have high gain, wide BW, are compact, and can be conveniently integrated with planar structures [17–19].

Furthermore, when arrays are used in MIMO configurations, the most important figure of merit is the correlation coefficient (CC). The CC describes the correlation or isolation of the communication channels when all the antennas are operated simultaneously. CC depends on the radiation patterns of the MIMO antenna elements and the propagation channel. The ideal desirable value of CC for best MIMO performance is zero. In literature, several ways were proposed to improve the CC, such as introducing physical distance between antenna elements [12–16], orienting the beams of antenna arrays in different directions or using different antenna polarisations. The physical distance isolates the beams but increases the overall size of the MIMO antenna system. On the other hand, beams can be oriented in different directions by the use of complex feeding networks [18, 20–23]. These feeding networks tilt the beam but increase the complexity, losses and overall size and cost of the antenna arrays and when used in MIMO configurations will enlarge the size significantly.

To tackle these problems, here, we propose to use SIW-based slot arrays in the place of microstrip antennas at mm-waves within a MIMO configuration of four elements. To have better CC, we will not introduce physical distancing between antenna elements or use complex feeding networks. However, we will design the SIW-based slot array so that the beams are oriented towards different directions and maintain these directions at all frequencies covered. So, although the antennas will be collocated (and share the same sidewall), acceptable CC is obtained, and as a result we can have a compact size MIMO antenna systems at mm-waves. This is because of the use of the simultaneous tilted beams. It should be noted that each array is designed such that it can be fed from either end to provide two beams of \pm of its beam tilts defined. As shown in the following sections (Table 3), the proposed design has a better

performance as compared to the designs available in the literature. It is compact in size, has simple feeding, provides an operating BW exceeding 4 GHz, and a maximum gain of 15 dBi. Hence, the proposed four-element MIMO configuration is well suited for 5G applications.

The study is organized as follows. Section 2 describes the theoretical background for the design of the travelling wave SIW slot array with the beam oriented along different directions. Section 3 presents the collocated MIMO antenna design details. The fabrication of the antenna and its measurement results are discussed in Section 4, and conclusions are presented in Section 5.

TABLE 1 Slot locations on the surface of the SIW

Slot	10° Tilt		30° Tilt	
	X (offset)	Z (position)	X (offset)	Z (position)
1	0.9851966	0	0.389826	0
2	−1.07025	4.829121	−0.73713	2.496656
3	0.9497578	10.03008	0.857617	5.889113
4	−0.8150907	14.62258	−0.88597	10.07596
5	1.396286	19.4348	1.254531	13.77265
6	−1.112776	25.26113	−1.10569	16.77637
7	1.204917	29.41418	1.261619	20.37165
8	−0.694599	34.86867	−0.88597	24.49089
9	0.666248	40.35697	1.034811	27.35939
10	0	42.88743	−0.78674	32.22231
12	—	—	−1.28288	38.26354
13	—	—	1.119864	42.38278
14	—	—	−0.00709	45.4541

Note: All the values are in mm.

Abbreviation: SIW, substrate integrated waveguide.

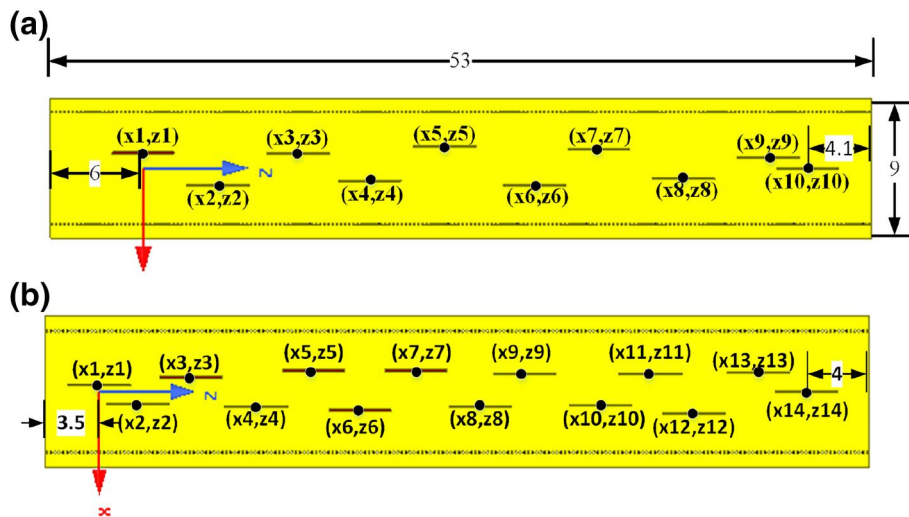


FIGURE 1 Substrate integrated waveguide antenna: (a) 10 slots producing 10° tilt; and (a) 14 slots producing 30° tilt

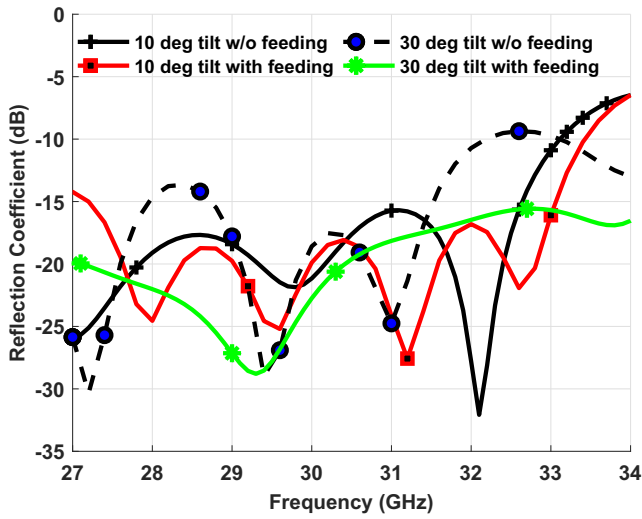


FIGURE 2 Reflection coefficient of the substrate integrated waveguide antenna

2 | SINGLE ANTENNA ELEMENT DESIGN

SIW slot arrays can either be of standing wave [17] or travelling wave [18, 19] types. Standing wave SIW arrays have radiation beams directed towards broadside, while travelling wave ones can direct the radiation beam in oblique directions. Numerous techniques have been proposed for designing such antennas in the literature, based on the design principles described in [24, 25], complex feed networks [17, 26], multi-layer [27] and planar arrays [28, 29]. All these methods are complex and have large sizes. Extending these designs methodologies to design MIMO antenna systems for mobile terminals at mm-waves will be difficult. Recently, a new design methodology for travelling wave rectangular waveguide arrays at mm-waves was presented in [30–34]. This methodology considered a simple feeding and can orient the beam in oblique directions. We will use the same methodology and apply it to design SIW-based slot arrays at mm-waves because SIW-based slot arrays can be easily integrated with other electronics.

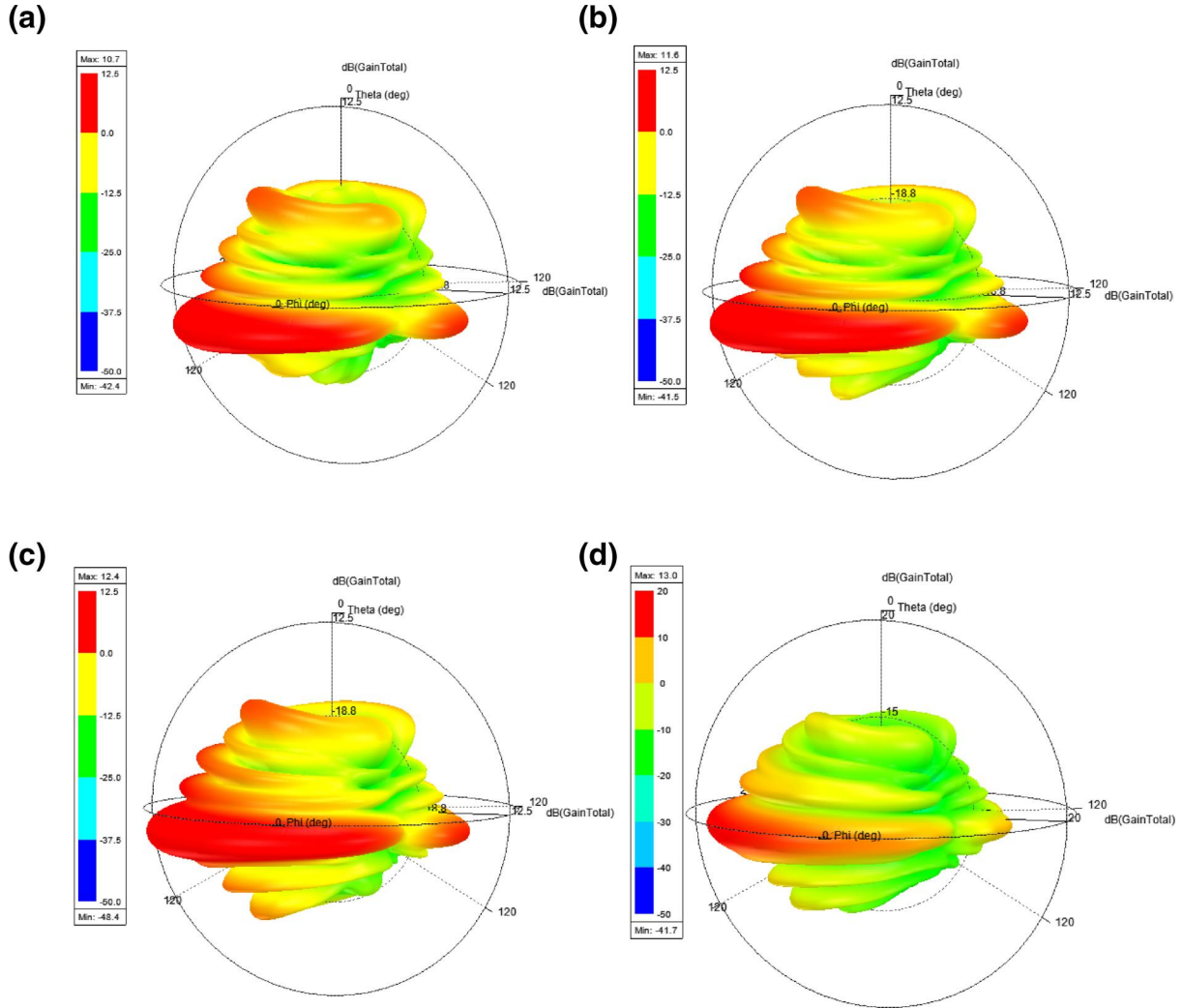


FIGURE 3 3D radiation patterns of substrate integrated waveguide antenna with a beam of 10° tilt at: (a) 29 GHz, (b) 30 GHz, (c) 31 GHz and (d) 32 GHz, respectively

The methodology to design an SIW-based slot array, with beams oriented towards the desired direction, is briefly discussed here. It is well known that by invoking the equivalence principle we can replace a slot with a magnetic dipole, which can in turn be replaced by an array of magnetic infinitesimal dipoles (IDs). An array of IDs are located at (x_d, y_d, z_d) and they are oriented along the angle (θ_d, ϕ_d) . At an observation point (x, y, z) , the \vec{E} and \vec{H} fields radiated by an array of N magnetic IDs can be expressed as [30–34],

$$\vec{E}(\mathbf{r}) = \sum_{n=1}^N \frac{c_o k_o^2}{4\pi} (\mathbf{n}_n \times \mathbf{P}_n) \cdot \frac{e^{-jk_o r_n}}{r_n} \quad (1)$$

$$\vec{H}(\mathbf{r}) = \sum_{n=1}^N \frac{1}{4\pi\epsilon_o} (k_o^2 (\mathbf{n}_n \times \mathbf{P}_n) \times \mathbf{n}_n) \cdot \frac{e^{-jk_o r_n}}{r_n} \quad (2)$$

where c_o is the speed of light in vacuum, k_o is the free space wave-number and \mathbf{n}_n represents the unit vector from the n th ID location to an observation point, and it can be expressed as

$$\mathbf{n}_n = \left(\frac{x - x_d(n)}{r_n}, \frac{y - y_d(n)}{r_n}, \frac{z - z_d(n)}{r_n} \right)^T \quad (3)$$

and the n th dipole moment (\mathbf{P}_n) is

$$\mathbf{P}_n = A_d(n) \cdot e^{j\phi_d(n)} \cdot \begin{pmatrix} \cos(\phi_d(n)) * \sin(\theta_d(n)) \\ \sin(\theta_d(n)) * \sin(\phi_d(n)) \\ \cos(\theta_d(n)) \end{pmatrix} \quad (4)$$

where $A_d(n)$ is the complex excitation of the n th dipole and r_n represents the distance between the observation point and the centre of the n th dipole. We employ a genetic algorithm (GA) by using the number of the slots, the desired radiation pattern, that is, direction and the side lobe level (SLL) as inputs, to determine the optimal locations of the slots on the top wall of the SIW. The cost function is the mean square error between the radiated and desired radiation patterns. The algorithm is run until either the desired radiation pattern is realised, or the preset maximum number of iterations has been reached.

Our objective is to design a four-element collocated MIMO antenna, whose beams point towards 10° , -10° , 30° and -30° . Please note that the objective behind tilting the beams was to achieve better values of CC and not to design a tilted array. Based on our observation, beam tilts of 30° , -10° , 10° and -30° provide good values of CC and we do not need to tilt the beams further. For the first antenna element, we choose our objective to realize a tilted beam pointing at 10° in elevation. We consider a 10-element SIW

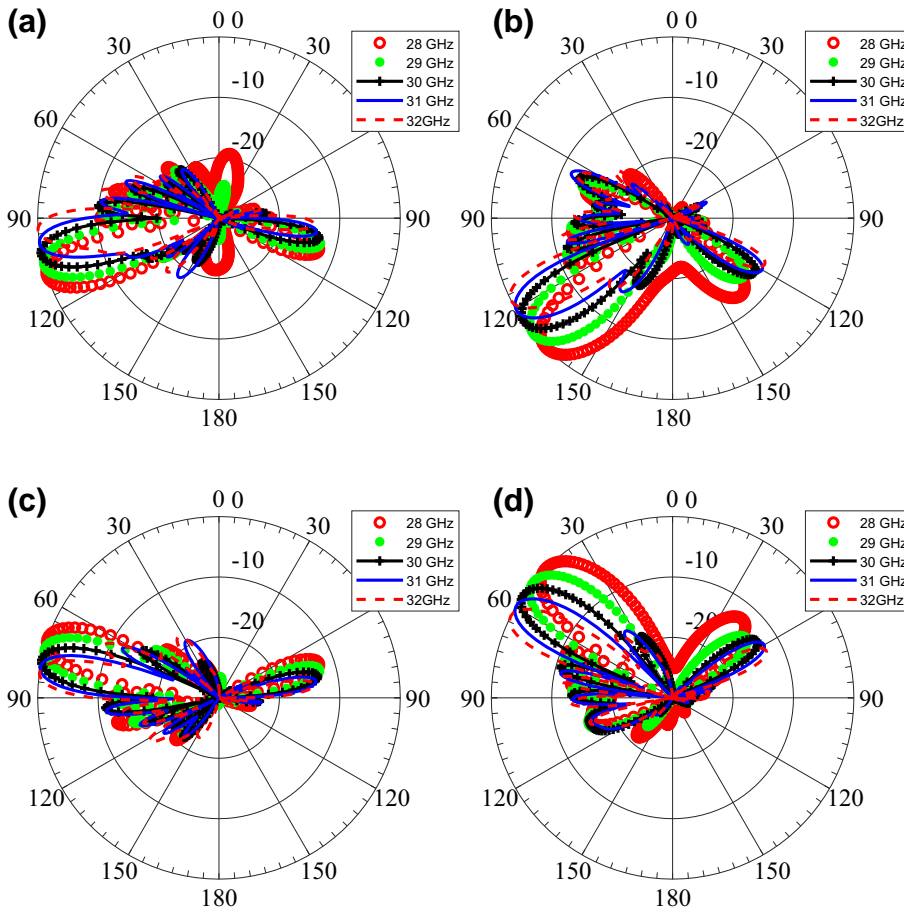


FIGURE 4 2D normalised radiation patterns with a 10° and 30° tilt for $\phi = 90^\circ$ cut at different frequencies in the absence of the microstrip to substrate integrated waveguide transition: (a) 10° tilt, (b) 30° tilt, (c) -10° tilt and (d) -30° tilt

slot array to achieve this goal. The GA determines the locations of the slots on the surface of the SIW as desired with an SLL of 11 dB. The geometry of the SIW antenna is shown in Figure 1(a). The width and length of the SIW slot antenna array were 7.3 and 53 mm, respectively. It was modelled on a Rohacell 51 IG-F foam substrate, whose thickness was 0.5 mm, and the distance between the first and last slot, and the ends of the SIW, were optimized using ANSYS-HFSS to improve the performance. Next, a 14-element slot array with a tilt angle of 30° was designed, as shown in Figure 1(b). The width and length of the 14-element slot array were also 7.3 and 53 mm, respectively. It was built on the same Rohacell substrate as above.

Table 1 shows the locations of the slots on the surface of the SIW for the two tilt angles. The reflection coefficient of the antenna is plotted in Figure 2. We can observe that the antenna has a relatively wide BW (27.5–32.5 GHz) based on the voltage standing wave ratio (VSWR) < 2.0 criterion. Figure 3 clearly shows a beam tilt of 10° from broadside at different frequencies. The 2D normalised radiation pattern at $\phi = 90^\circ$ cut is shown in Figure 4a. The tilt in the main beam changes with frequency because of the travelling wave behaviour of the antenna. Since, this affects all the elements, the relative tilts are still maintained as we change the frequency.

Feeding the antenna is a challenging task at mm-waves and the performance of the antenna depends significantly on how it is fed. In the present design, a microstrip to the SIW transition was placed at both ends of the SIW slot array. The transition was optimized for the reflection coefficient and the radiation patterns desired tilts. The geometry of the SIW antenna with its feed transitions is shown in Figure 6a, while the reflection coefficient and the radiation pattern of the antenna are presented in Figures 2 and 5a, respectively. Based on the VSWR < 2.0 criterion, we found that the BW performance is not affected significantly by the microstrip-to-SIW transition, though, it does affect the SLL.

The design of a SIW slot antenna with a tilt of 30° and low SLL is even more challenging because it becomes increasingly difficult to control the SLL when the tilt angle is high. We observe that the separation distance between the slots for the 30° tilt case is less than the 10° case; consequently, we increased the number of slots while keeping in mind the length constraints that should remain unchanged from the case of Antenna 1 (10° case). A total of 14 slots are found to produce a tilt of 30° over a wide band, while meeting the length (SIW size) criterion. The geometry of the proposed 14 slot array is shown in Figure 1(b). The reflection coefficient and the radiation pattern of the antenna are plotted in Figures 2 and 4b,

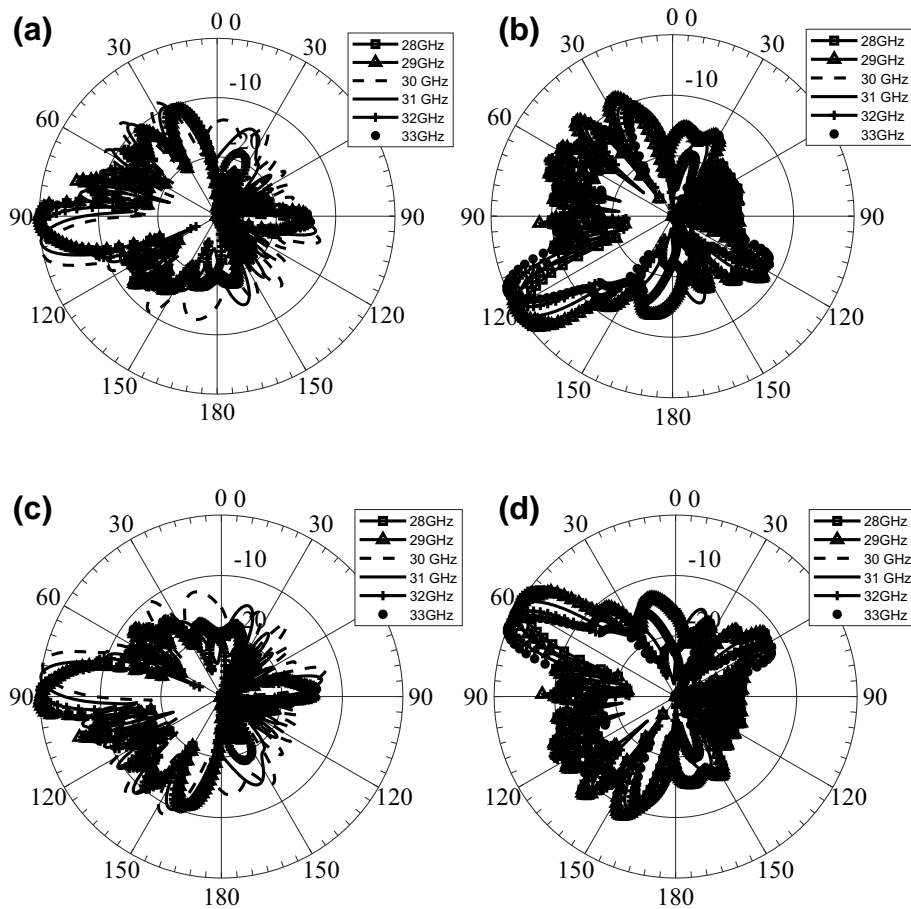


FIGURE 5 2D normalised radiation patterns with a 10° and 30° tilt for $\phi = 90^\circ$ cut at different frequencies in the presence of the microstrip to SIW transition: (a) 10° tilt, (b) 30° tilt, (c) -10° tilt and (d) -30° tilt. SIW, substrate integrated waveguide

respectively. We can also observe a slight shift in the antenna beam maximum with respect to frequency. A microstrip to SIW transition was used to feed the antenna and was optimized based on the reflection coefficient and the radiation patterns. The geometry of the proposed antenna along with the

microstrip-to-SIW transition is shown in Figure 6b. The reflection coefficient and the radiation pattern are shown in Figures 2 and 5b, respectively. The SLL was around 8.5 dB.

To realize a tilt in the negative direction, that is, -10° and -30° are relatively straight forward, since the antenna has two

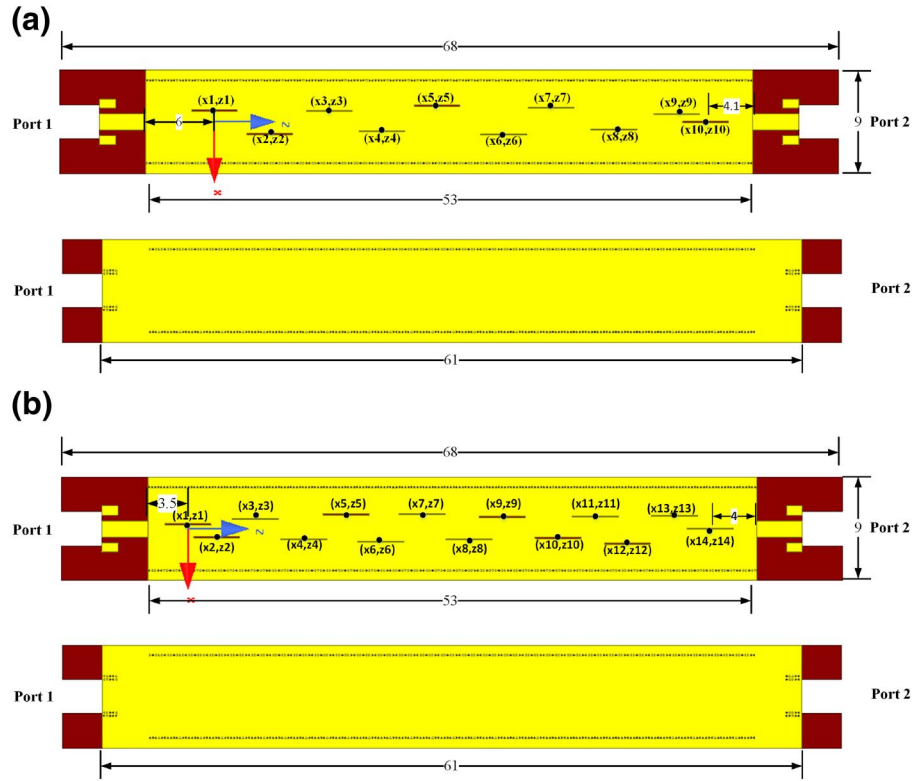


FIGURE 6 Top and bottom views of the substrate integrated waveguide antenna: (a) 10 slots producing 10° tilt and (b) 14 slots producing 30° tilt

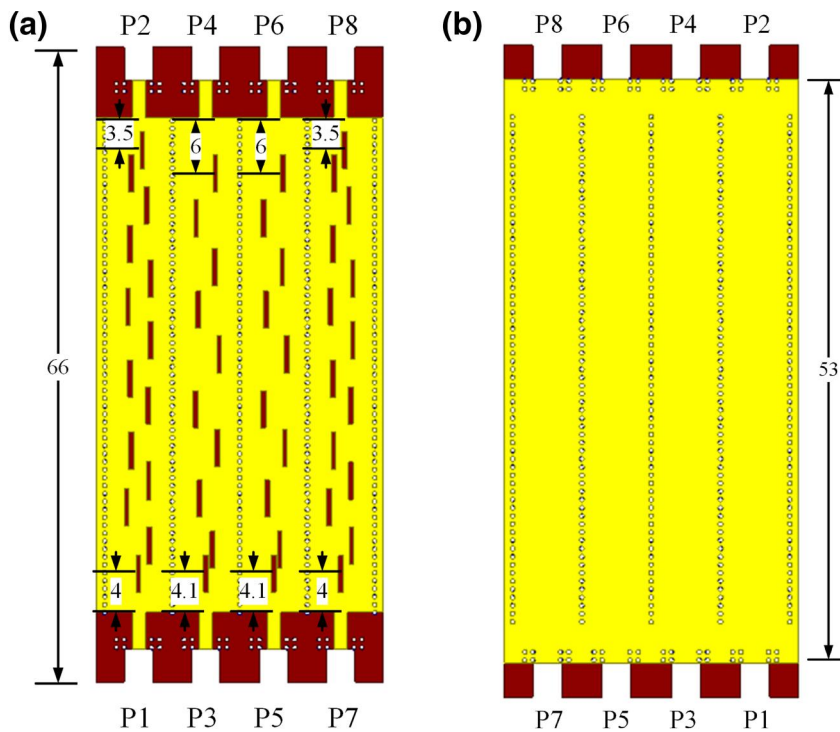


FIGURE 7 Four element collocated multiple-input multiple-output antenna design: (a) top view and (b) bottom view. All dimensions are in mm

feed points. The antenna is typically fed from the left while the other side (right) is terminated with a matched load. To tilt the beam in the backward direction, for example, -10° , we feed the antenna from the opposite end, that is, from port 2, as shown in Figure 4c and d. This gives an added feature of beam control and dynamic change when needed.

3 | FOUR-ELEMENT MIMO

Following the design of single antenna elements with beam tilt angles of 10° and 30° , accompanied by a wide BW and acceptable SLL performance, we designed a collocated four-element MIMO antenna with adjacent elements sharing the via walls. Our goal is to have the smallest possible antenna, so that it is suitable for future wireless terminals and access points.

The geometry of the proposed antenna is shown in Figure 7, where the first antenna element produces a tilt of

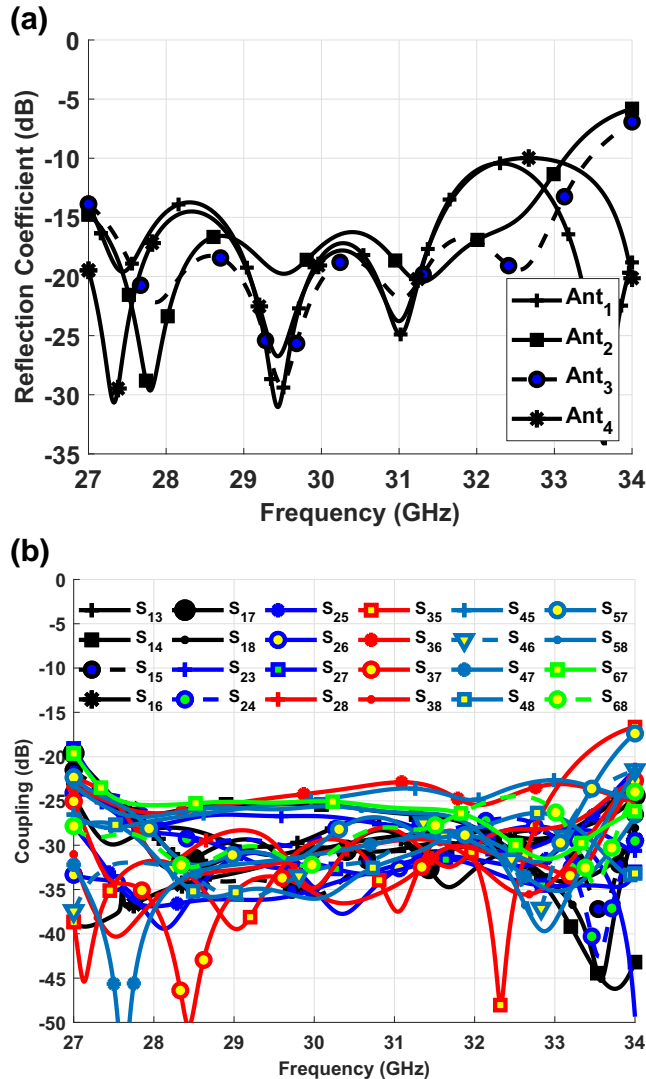


FIGURE 8 Reflection and isolation curves of the four element collocated multiple-input multiple-output antenna design: (a) simulated reflection coefficient and (b) simulated isolation curves

-30° , second $+10^\circ$, third -10° while the fourth has a tilt of $+30^\circ$, all with respect to broadside. The collocated placement of the antennas affect their performance in terms of the BW, SLL level and radiation. The distance between the slot and the edge of the SIW, as well as the slot positions, were optimized for the reflection coefficient and the radiation pattern with a view to improve the performance of the antennas. The proposed design focused on somehow fixed beams from the arrays to guarantee low correlation between them at all covered frequencies and to maintain small size and enough operating BW. The design can be modified to have wider scanning beams, but a trade-off will be made.

The reflection coefficients and the coupling performance of the four-element MIMO antenna design are presented in Figures 8a and b, respectively. We can observe that all the MIMO antenna elements have an impedance BW ranging from 27 to 33 GHz. The antenna elements have very good isolation, better than 20 dB. The radiation patterns of all the four elements are shown in Figure 9 for the $\phi = 90^\circ$ cut at the three frequencies of 30, 31 and 32 GHz. The SLLs of the antennas in the middle are affected more compared to those of the neighbouring antennas, and a possible reason for this degradation is the presence of the collocated antenna on both sides of the middle section and sharing of the via walls. Figures 9b and c show the degradation of the SLL.

The CC can be calculated as [35].

$$\rho_{ij} = \frac{\left| \iint_{4\pi} \vec{F}_i(\theta, \phi) * \vec{F}_j(\theta, \phi) d\Omega \right|}{\left| \iint_{4\pi} \vec{F}_i(\theta, \phi) d\Omega \right| \left| \iint_{4\pi} \vec{F}_j(\theta, \phi) d\Omega \right|} \quad (5)$$

where $\vec{F}_i(\theta, \phi)$ represents the 3D-radiation pattern, when i th port is excited, the $*$ is the Hermitian product and Ω represents the solid angle. The CC calculation between the MIMO antenna elements at different frequencies is presented in Table 2. The values obtained from the field correlation calculation are well below the desired limit and it is due to the beam tilt. The gain and efficiency of the antenna elements are presented in Figures 10(a) and (b), respectively. We observe that the gain varies between 14 and 16.5 dBi, across the 3 GHz BW.

The novelty of our proposed design compared to the existing ones (available in the literature) is shown in Table 3. It is the most compact design as there is no separation distance between adjacent MIMO antennas (they use same sidewalls). Furthermore, it offers the highest gain as compared to all the available MIMO designs in the literature. It should be noted that the design was optimized for having at worst a 3-dB gain variation within the BW of interest and not for the widest impedance BW. In addition, it provides four-tilted beams without the use of a feeding network (i.e. Butler matrix) with the possibility of being fed from both sides. For MIMO antennas, the SLL is not an important figure of merit, that is, why the majority of previous works did not focus on it. For MIMO antennas, spatial correlation of the antenna is the most important parameter of

performance evaluation, but for collocated MIMO antenna elements, if the SLL is close to the level of the main lobe, then the CC value will be high and, as a result, a poor MIMO performance will be obtained. As long as the beams are uncorrelated, the MIMO antenna system will enhance the channel capacity (in an isotropic environment).

4 | FABRICATION AND MEASUREMENTS

The fabrication of the four-element SIW slot array with collocated MIMO design was a challenging task because it required a large number of vias in a very confined region. To handle this problem, we used a Rohacell 51 IG-F foam of 0.5 mm thickness. To introduce top and bottom metal surfaces on a Rohacell 51 IG-F foam, we used an adhesive material 3M VHB double-sided tape, whose thickness was 0.025 mm. Dupont AP 8525 is a flexible polyimide material (Kapton) that was used between the adhesive and copper with a thickness of 0.05 mm. A 0.035-mm layer of copper plated on both sides was added. The layered view of the geometry is shown in Figure 11. Furthermore, instead of using vias, we used a via wall to connect the different layers, as well as act as a barrier between the MIMO antenna elements.

This is because it is not possible to create a large number of vias within the Rohacell. To address this issue, a via wall was built with a Rogers 5880 substrate with a thickness of 0.381 mm, which was plated with copper strips (0.017 mm thickness) on both sides to represent the vias.

The fabrication process consisted of several steps. Initially, we cut a flexible laminate and applied a photosensitive film on the top side of the material. After exposing and developing the film, features of the top and bottom were etched on two different pieces of the material. The off-the-shelf Rohacell foam 51 IG-F material, whose thickness was 1 mm, was machined down to 0.5 mm. Then, the internal layers of the

TABLE 2 Correlation coefficient

Freq	CC ₁₂	CC ₁₃	CC ₁₄	CC ₂₃
29.5	0.013612	0.010105	0.002383	0.007699
30	0.003373	0.020323	0.000729	0.001414
31	0.000816	0.033474	0.010409	0.014979
32	0.000347	0.011153	0.007682	0.017815
32.5	0.003818	0.00084	0.004542	0.00189

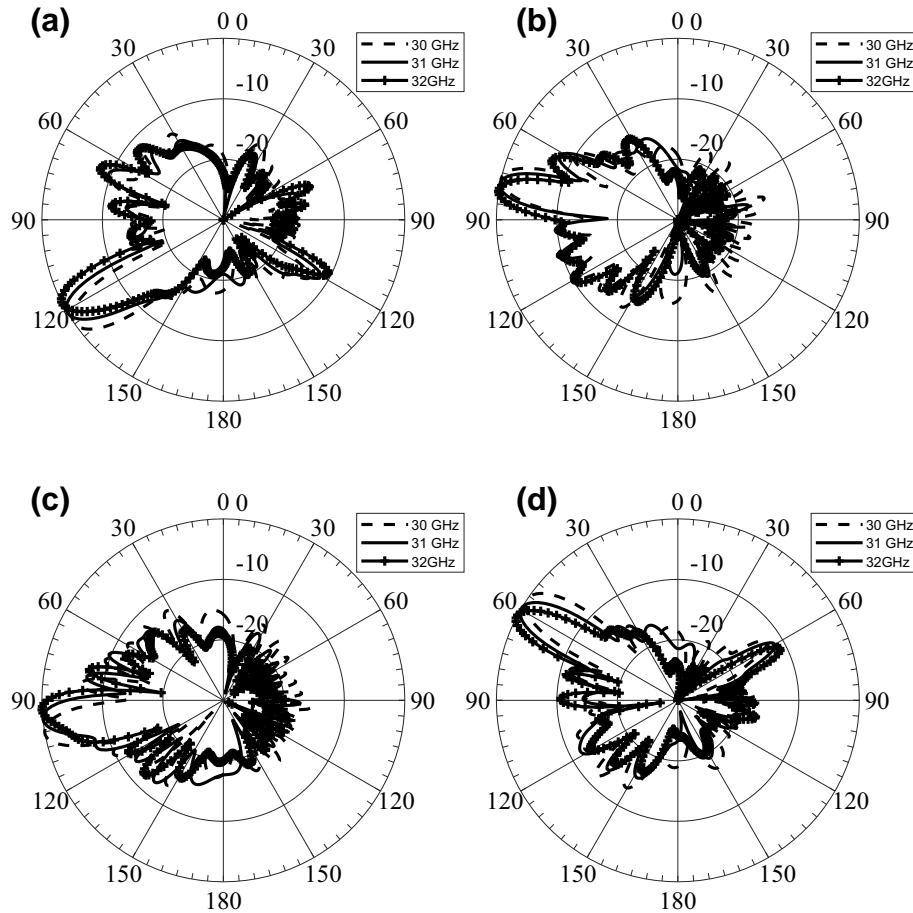


FIGURE 9 2D normalised radiation patterns for the $\phi = 90^\circ$ cut at 30, 31 and 32 GHz, and four cases: (a) Ant-1 (T1 excited), (b) Ant-2 (T4 excited), (c) Ant-3 (T5 excited) and (d) Ant-4 (T8 excited)

polyimide were coated with 3M VHB double-sided tape. The top and bottom layers were bonded to the Rohacell foam 51 IG-F. Next, the via wall was fabricated by using the Roger 5880 substrate with a copper layer etched on both sides, which was machined by using a special jig (or you can use tool) designed for this type of job. Then the strips were soldered on both

sides to connect the top and bottom sides. Solder wires were placed next to the connector position through the holes. Connectors (mini-SMPs) were soldered and the entire design was cleaned in an isopropyl alcohol bath. The fabricated geometry of the four-element co-located MIMO SIW design is shown in Figure 12.

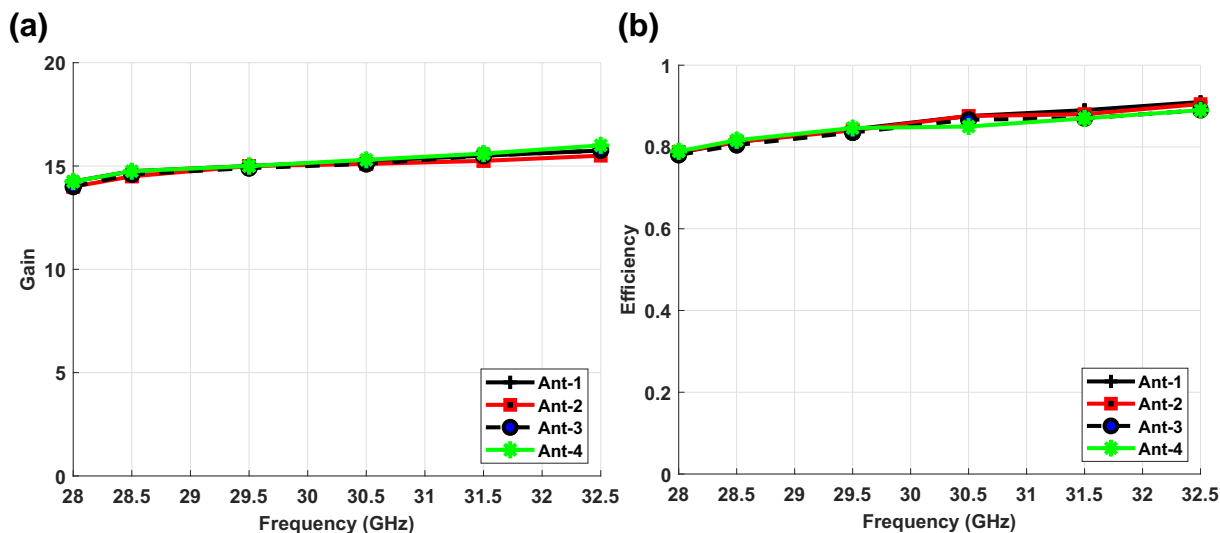


FIGURE 10 Simulated: (a) gain and (b) efficiency, when different antenna elements are excited at different frequencies

TABLE 3 Comparison of our proposed design with other MIMO designs available in the literature at mm-waves (28 GHz), where WB, NP and SM represent the wideband, not presented and same as the main lobe, respectively

Reference	Ant. type	No. of Ant elements	Ant. Sep	Dimensions (mm ³)	Freq. of operation	Freq. BW (GHz)	SLL (dB)	Gain (dBi)	ECC
[3]	Patch with slots	4	$0.75\lambda_0$	$19 \times 19 \times 9.6$	28	WB	NP	13	Location placement
[4]	H-shaped patch + EBG	8	$>1\lambda_0$	$31.2 \times 31.2 \times 1.57$	28	10.7%	SM	8.7	Location + EBG structure
[5]	SIW slot	4	$>1.5\lambda_0$	$72 \times 17.2 \times 1.575$	28	05.7%	7	11	Separation distance
[8]	PIFA	4	$>2\lambda_0$	$130 \times 68 \times 0.76$	28	03.6%	6	12	Location placement
[10]	Bow tie	2	$>1\lambda_0$	$130 \times 65 \times 0.5$	28	WB	NP	12.4	Location placement
[11]	T-shaped Patch + DGS	4	Different grounds	$55 \times 22 \times 0.8$	28	WB	SM	5 at 28 GHz, 10.5 at 36 GHz	Location placement
[13]	Connected array	2	$>2\lambda_0$	$100 \times 60 \times 0.76$	18	04.6%	NP	8	Location placement
[14]	Connected array	2	$>2\lambda_0$	$115 \times 65 \times 0.76$	28	17.14%	SM	9.9	Location placement
[16]	Tapered slot	4	$>2\lambda_0$	$104 \times 104 \times 0.51$	28	WB	SM	11	Location placement
Our proposed	SIW slot	4	0	$68 \times 30.68 \times 0.5$	28	14.5%	7	15	Spatial isolation

Abbreviations: BW, bandwidth; MIMO, multiple-input multiple-output; SIW, substrate integrated waveguide; SLL, side lobe level.

The measured reflection and isolation curves of the collocated four-element MIMO antenna design are shown in Figures 13(a) and (b), respectively. We can observe a slight difference between the measured and the simulated results, this can be attributed to fabrication errors introduced by the sequential fabrication steps. The radiation patterns were measured in a mm-wave far-field chamber at the Polytechnique

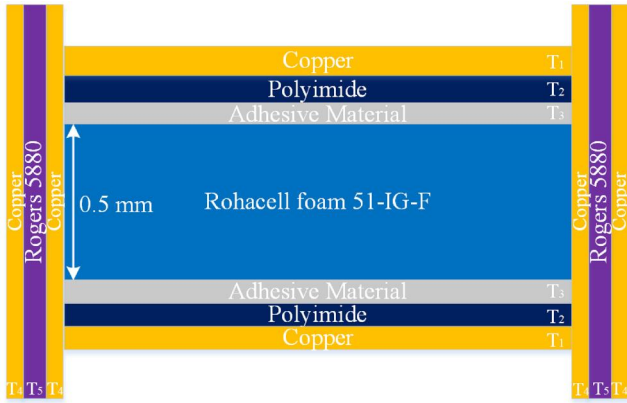


FIGURE 11 Layered view of the fabricated geometry. The thickness T_1 to T_5 are 0.035, 0.05, 0.025, 0.017 and 0.381 mm, respectively

Montreal, and the measurement setup is shown in Figure 14. Figure 15 presents the measured radiation patterns for the same cut as that in Figure 9. In the worst scenario, SLL was around 6 dB but still acceptable CC values were achieved. Note that only the front half of the pattern is presented because of the limitation imposed by the measurement setup, which only covered the upper hemisphere. We observe that the main beam is in the desired direction, but there is a slight increase in the SLL. The measured gain levels were close to those predicted by the simulations (ranged between 14 and 15 dBi). We believe that the fabrication tolerances are responsible for the differences between the simulated and measured results, and a slight bend in the material may also have contributed to these differences.

5 | CONCLUSIONS

A four-element, collocated travelling wave SIW MIMO antenna operating at mm-waves has been presented in this work. Each element of the antenna system is composed of slot arrays whose radiated beams tilt along different angles in space to provide low correlation. The antenna elements have all been designed to cover the BW of 4 GHz ranging from 28 to

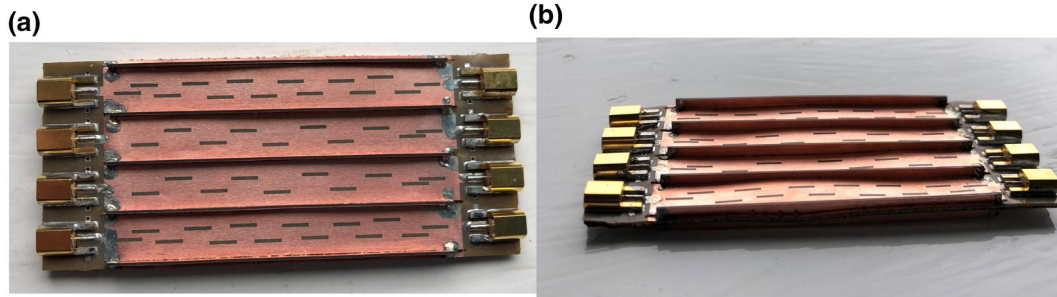


FIGURE 12 Fabricated geometry: (a) top view and (b) side view

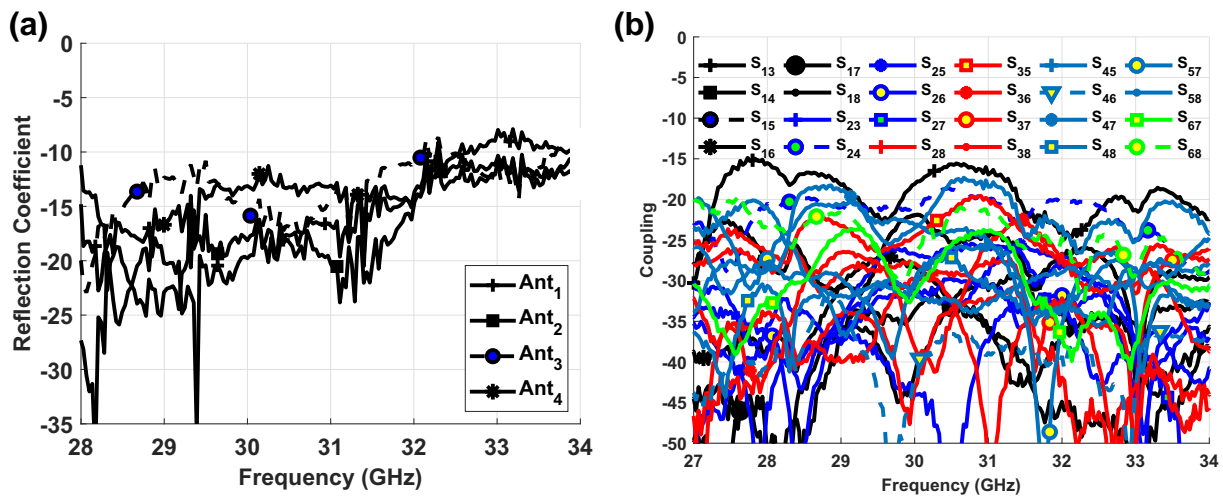


FIGURE 13 The reflection and isolation curves of the four element collocated multiple-input multiple-output antenna design: (a) measured reflection coefficient and (d) measured isolation curves

32 GHz. The measured gain value of the antenna element varied between 14 and 15 dBi across the operating bands. Even though the antennas are collocated, the isolation is shown to be better than 20 dB for all combinations of the antenna elements, which is desirable. The proposed design is suitable for future mm-waves enabled terminals.

ACKNOWLEDGEMENTS

The authors would like to thank Kirill Klionovski (KAUST) and Mohammad Reza Rahimi (Polytechnique Montreal) for their help in testing the antenna. This study was partially funded by KFUPM DSR Project no. FT 161006 and KAUST Project on ST-2016-KKI-2899.

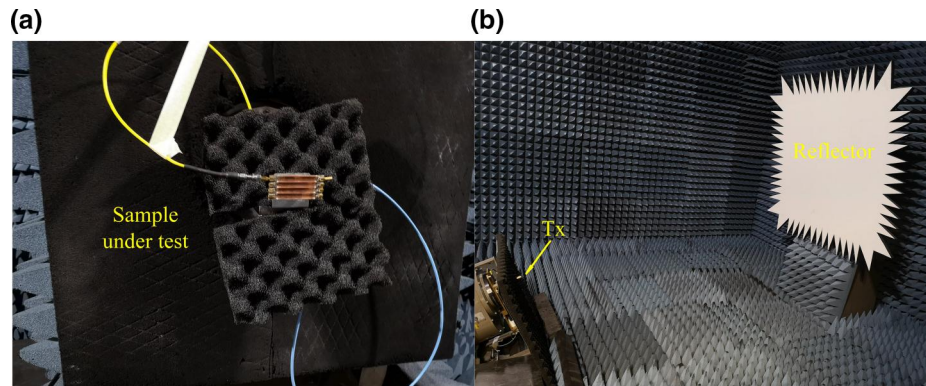


FIGURE 14 Radiation pattern measurement setup: (a) sample under test and (b) source antenna and reflector for plane wave generator

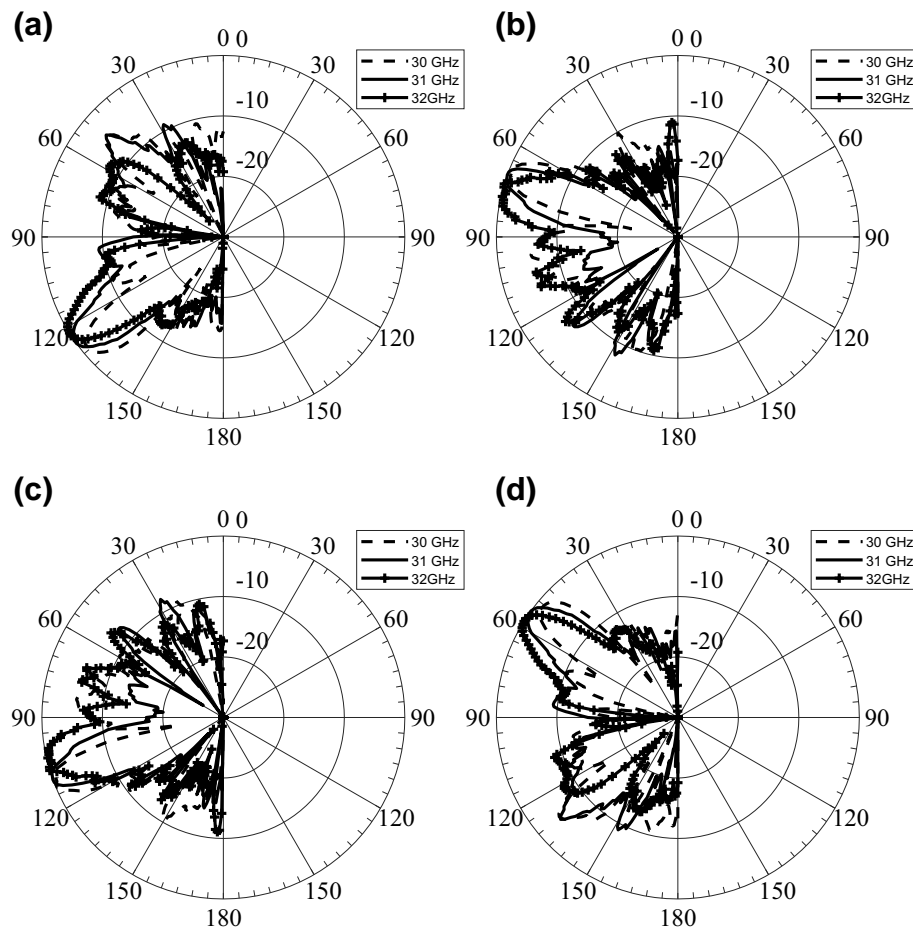


FIGURE 15 Measured 2D normalised radiation patterns for $\phi = 90^\circ$ cut at three frequencies: 30, 31 and 32 GHz: (a) Ant-1 (T1 excited), (b) Ant-2 (T4 excited), (c) Ant-3 (T5 excited) and (d) Ant-4 (T8 excited)

ORCID

Asim Ghalib  <https://orcid.org/0000-0001-6503-2394>

Hussein Attia  <https://orcid.org/0000-0002-6407-9251>

REFERENCES

- Sharawi, M.S.: Printed MIMO Antenna Engineering. Artech House, Norwood (2014)
- Qingling, Z., Li, J.: Rain attenuation in millimetre wave ranges. In: Proceedings of the 7th International Symposium on Antennas, Propagation & EM Theory, Guilin, pp. 1–4 (2006)
- Hussain, N., et al.: A broadband circularly polarized fabry-perot resonant antenna using a single-layered PRS for 5G MIMO applications. *IEEE Access*, 7, 42897–42907 (2019)
- Shoab, N., et al.: MIMO antennas for smart 5G devices. *IEEE Access*, 6, 77014–77021 (2018)
- Lin, M., et al.: Gain-enhanced Ka-band MIMO antennas based on the SIW corrugated technique. *IEEE Antennas Wirel. Propag. Lett.* 16, 3084–3087 (2017)
- Haraz, O.M., et al.: Single-band PIFA MIMO antenna system design for future 5G wireless communication applications. In: Proceedings of the IEEE 11th International Conference on Wireless and Mobile Computing, Networking and Communications (WiMob), Abu Dhabi, 608–612 (2015)
- Hashem, K., et al.: 6-Element 28/38 GHz dual-band MIMO PIFA for future 5G cellular systems. In: Proceedings of the IEEE International Symposium on Antennas and Propagation (APSURSI), Fajardo, 393–394 (2016)
- Ikram, M., et al.: A novel connected PIFA array with MIMO configuration for 5G mobile applications. In: Proceedings of the Australian Microwave Symposium (AMS), Brisbane, QLD, 19–20 (2018)
- Ojaroudiparchin, N., et al.: Multi-layer 5G mobile phone antenna for multi-user MIMO communications. In: Proceedings of the 23rd telecommunications forum TELFOR (TELFOR), Belgrade, 559–562 (2015)
- Parchin, N.O., et al.: End-fire phased array 5G antenna design using leaf-shaped bow-tie elements for 28/38 GHz MIMO applications. In: Proceedings of the IEEE international conference on ubiquitous wireless broadband (ICUWB), Nanjing, 1–4 (2016)
- Jilani, S.F., Alomainy, A.: Millimetre-wave T-shaped MIMO antenna with defected ground structures for 5G cellular networks. *IET Microw. Antennas Propag.* 12(5), 672–677 (2018)
- Naqvi, S.I., et al.: An integrated antenna system for 4G and millimetre-wave 5G future handheld devices. *IEEE Access*, 7, 116555–116566 (2019)
- Sharawi, M.S., et al.: A two concentric slot loop based connected array MIMO antenna system for 4G/5G terminals. *IEEE Trans. Antennas Propag.* 65(12), 6679–6686 (2017)
- Ikram, M., et al.: A multiband dual-standard MIMO antenna system based on monopoles (4G) and connected slots (5G) for future smart phones. *Microw. Opt. Technol. Lett.* 60, 1468–1476 (2018)
- Hussain, R., et al.: Compact 4G MIMO antenna integrated with a 5G array for current and future mobile handsets. *IET Microw. Antennas Propag.* 11(2), 271–279 (2017)
- Ikram, M., et al.: Multiband MIMO microwave and millimetre antenna system employing dual-function tapered slot structure. *IEEE Trans. Antennas Propag.* 67(8), 5705–5710 (2019)
- Xu, J.F., et al.: Design and implementation of low sidelobe substrate integrated waveguide longitudinal slot array antennas. *IET Microw. Antennas Propag.* 3(5), 790–797 (2009)
- Hosseininejad, S.E., Komjani, N.: Optimum design of travelling-wave SIW slot array antennas. *IEEE Trans. Antennas Propag.* 61(4), 1971–1975 (2013)
- Ghalib, A., et al.: Broadband substrate integrated waveguide slotted array antenna at mm-wave bands. In: Proceedings of the IEEE MTT-S international microwave workshop series on 5G hardware and system technologies (IMWS-5G), Ireland (2018)
- Chen, C., Chu, T.: Design of a 60-GHz substrate integrated waveguide Butler matrix—a systematic approach. *IEEE Trans. Microw. Theor. Tech.*, 58(7), 724–733 (2010)
- Cheng, Y.J., et al.: Substrate integrated waveguide (SIW) Rotman lens and its Ka-band multibeam array antenna applications. *IEEE Trans. Antennas Propag.* 56(8), 2504–2513 (2008)
- Chen, P., et al.: A double layer substrate integrated waveguide Blass matrix for beamforming applications. *IEEE Microw. Wirel. Compon. Lett.* 19(6), 374–376 (2009)
- Djerafi, T., et al.: Planar Ku-band 4 x 4 Nolen matrix in SIW technology. *IEEE Trans. Antennas Propag.* 58(2), 259–266 (2010)
- Mallahzadeh, A., Mohammad-Ali-Nezhad, S.: A low cross-polarization slotted ridged SIW array antenna design with mutual coupling considerations. *IEEE Trans. Antennas Propag.* 63(10), 4324–4333 (2015)
- Yan, L., et al.: Simulation and experiment on SIW slot array antennas. *IEEE Microw. Wirel. Compon. Lett.* 14(9), 446–448 (2004)
- Yang, H., et al.: Improved design of low sidelobe substrate integrated waveguide longitudinal slot array. *IEEE Antennas Wirel. Propag. Lett.* 14, 237–240 (2015)
- Qiu, L., et al.: A double-layer shaped-beam travelling-wave slot array based on SIW. *IEEE Trans. Antennas Propag.* 64(11), 4639–4647 (2016)
- Zhang, L., et al.: Design of a travelling wave slot array on substrate integrated waveguide for 24GHz traffic monitoring. In: Proceedings of the cross strait quad-regional radio science and wireless technology Conference (CSQRWC), Xuzhou, pp. 1–3 (2018)
- Hosseininejad, S.E., et al.: Accurate design of planar slotted SIW array. *IEEE Antennas Wirel. Propag. Lett.* 14, 261–264 (2015)
- Clauzier, S., et al.: A new method for the design of slot antenna arrays: theory and experiment. In: Proceedings of the 10th European conference on antennas and propagation (EuCAP), Switzerland (2016)
- Sarkar, D., et al.: An efficient analytical evaluation of the electromagnetic cross correlation Green's function in MIMO systems. *IEEE Trans. Antennas Propag.* 67(11), 6947–6956 (2019)
- Mikki, S., et al.: Near-field cross-correlation analysis for MIMO wireless communications. *IEEE Antennas Wirel. Propag. Lett.* 18(7), 1357–1361 (2019)
- Mikki, S.M., et al.: A Novel Slot Antenna Array Synthesis Algorithm for Reconfigurable Beamforming. (2019). https://www.researchgate.net/publication/332445544_A_Novel_Slot_Antenna_Array_Synthesis_Algorithm_for_Reconfigurable_Beamforming
- Mikki, S., Antar, Y.: On cross correlation in antenna arrays with applications to spatial diversity and MIMO systems. *IEEE Trans. Antennas Propag.* 63(4), 1798–1810 (2015)
- Sharawi, M.S., et al.: Correlation coefficient calculations for MIMO antenna systems: a comparative study. *Int. J. Microw. Wirel. Technol.* 9(10), 1991–2004 (2017)

How to cite this article: Ghalib A, Sharawi MS, Mittra R, Attia H, Shammim A. Collocated MIMO travelling wave SIW slot array antennas for millimetre waves. *IET Microw. Antennas Propag.* 2021;15:815–826. <https://doi.org/10.1049/mia2.12110>